

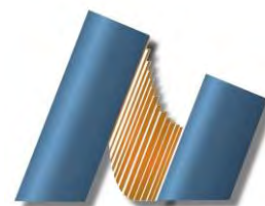


UNIVERSIDAD NACIONAL AUTÓNOMA DE MÉXICO

CENTRO DE NANOCIENCIAS Y NANOTECNOLOGÍA

LICENCIATURA EN NANOTECNOLOGÍA

(Nanofabricación y microelectrónica)



“Desarrollo de un sistema Biofotónico con un Laser Diodo para la obtención de imágenes de microorganismos vivos en una celda”

“Development of a Biophotonic System with a Laser Diode for Imaging Living Microorganisms in a Cuvette “

Tesis

QUE PARA OPTAR POR EL TÍTULO DE:

LICENCIADO EN NANOTECNOLOGÍA

PRESENTA:

Marino Alberto Lara Alva

DIRECTORES DE TESIS

Dra. Veneranda Guadalupe Garcés Chávez and Dr. Kevin O'Donnell

ENSENADA, BAJA CALIFORNIA (Agosto) 2018



Universidad Nacional
Autónoma de México



UNAM – Dirección General de Bibliotecas
Tesis Digitales
Restricciones de uso

DERECHOS RESERVADOS ©
PROHIBIDA SU REPRODUCCIÓN TOTAL O PARCIAL

Todo el material contenido en esta tesis esta protegido por la Ley Federal del Derecho de Autor (LFDA) de los Estados Unidos Mexicanos (México).

El uso de imágenes, fragmentos de videos, y demás material que sea objeto de protección de los derechos de autor, será exclusivamente para fines educativos e informativos y deberá citar la fuente donde la obtuvo mencionando el autor o autores. Cualquier uso distinto como el lucro, reproducción, edición o modificación, será perseguido y sancionado por el respectivo titular de los Derechos de Autor.

Hago constar que el trabajo que presento es de mi autoría y que todas las ideas, citas textuales, datos, ilustraciones, gráficas, etc. sacados de cualquier obra o debidas al trabajo de terceros, han sido debidamente identificados y citados en el cuerpo del texto y en la bibliografía y acepto que en caso de no respetar lo anterior puedo ser sujeto de sanciones universitarias.

Afirmo que el material presentado no se encuentra protegido por derechos de autor y me hago responsable de cualquier reclamo relacionado con la violación de derechos de autor.

Marino Alberto Lara Alva

Acknowledgements

I would like to start thanking the person that made all of this possible, my dad. Thanks to him I had all the tools to get where I am. The idea of providing me opportunities that he was not able to get, gave me the abilities to overcome all the barriers that I have faced until now. Even though he always had a hard time trying to communicate with me, he always helped me in everything he could. Every time I misbehaved he was hard on me and even though sometimes he overreacted, I always knew that he had a reason for doing it. I thank him for all of his support and love.

Thank you mother for always been there. Thank you for always skyping with me every weekend. During my childhood you always helped me with my school affairs. Thanks to you, I waked every morning for school, too bad I never got used to it after more than 10 years. You always took care of me when I was sick or had an injury. You are as important as my dad, without both of you I would never have gotten this far. Finally, thank you for giving me the most important gift, life.

Special thanks to Monica, Juan, José and Laura for receiving and treating me as a family member even though we are not blood related. Sharing meal time with you felt like home. Thank you for offering your help every time I needed. I really appreciate all of you and consider as a family.

I would like to thank the Dr. Veneranda's and Dr. O'Donnell's group for all of your support during this project. At first, when I wanted to work with you I thought I would get rejected for my lack of knowledge but I was wrong and I am very thankful for receiving me. Special thanks to Dr. Veneranda because she made possible that I could work with this group. Dr. Veneranda supported me in all she could during this project and always was available when I needed her help, which is something that I really appreciate. Thank you Daniel and Beatriz for helping me; you were already busy and still shared time with me. I learned a lot being with this group and I am very thankful for that.

Lastly I would like to thank my friends from college and my roommates. I had great times with all of my college friends because we shared many experiences. I always felt supported by them and every time I needed help, they were always there for me. Not only they were my college friends but they were a family. During my stay in Ensenada I had multiple roommates, some of them leaved because they found a cheaper flat and others because they could only stay for 6 months. Each and every one of them were important because their presence always made my day feel joyful and warm.

Thank you all for guiding me and always supporting me. You all give me the strength to move forward and never give up no matter how hard things get.

Resumen:

En esta tesis se construyó un sistema biofotónico con el propósito de observar microorganismos vivos dentro de una celda, en específico la microalga *Dunaliella tertiolecta* (Dt). El sistema se compone de tres módulos: módulo de iluminación, detección y de muestra. Antes de la construcción del sistema, se necesitó caracterizar ópticamente un láser diodo. Se obtuvo tanto la potencia de salida, así como espectro para diferentes valores en el regulador de corriente. Se obtuvo también el tamaño del perfil del haz y como este cambiaba durante su propagación. Antes de observar las muestras de Dt en la celda, el sistema se probó con muestras preparadas en porta objetos. Con el sistema biofotónico fue posible generar imágenes y videos dentro de la celda. Las imágenes y los videos se obtuvieron mediante el uso de la técnica de campo brillante y de fluorescencia. En conjunto con lo anterior, fue posible generar y observar corrientes convectivas al enfocar el láser diodo de 406.5-407.5 nm y con una potencia de 20 y 50 mW. El sistema fue diseñado para ser versátil para el estudio de una gran variedad de muestras biológicas dentro de una celda.

Abstract:

In this thesis a biophotonic system was built in order to observe living microorganisms such as *Dunaliella tertiolecta* (Dt) microalgae cells inside a cuvette. The system is composed of three modules: illumination, detection, and sample module. Before building the system, an optical characterization for a laser diode was required. The output power and spectra for different drive currents were measured, as well as the beam profile and the evolution of the beam propagation. Before observing the Dt sample in a cuvette, the system was tested using thin chamber samples. With the system it was possible to generate images and videos inside the cuvette. The images and videos were obtained by using the brightfield technique and fluorescence. In addition to the imaging and recording, it was possible to generate and observe convective flux by focusing strongly a laser diode of 406.5-407.5 nm with 20 and 50 mW. The system was design to be versatile to studying a great variety of biological samples inside a cuvette.

Index

1. Introduction	1
2. Background	2
2.1. Illumination Module	2
2.1.1. Brightfield Microscopy	3
2.1.2. Fluorescence	3
2.1.4. Laser Diode (LD)	3
2.1.5. Laser Diode optical characterization	5
2.1.6. Spectrometer	5
2.1.7. Use of speckle Pattern to find the laser diode's focal plane	6
2.2. Detection Module	6
2.2.1. Infinity corrected microscope objectives	6
2.2.2. CMOS camera	7
2.2.3. Optical Filters	7
2.3. Sample Module.....	7
2.3.1. <i>Dunaliella tertiolecta</i> (Dt)	8
2.4. Photothermal heating	8
3. Hypothesis	8
4. Objectives	8
5. Material and methods	9
5.1. Electronic assembly of a laser diode	9
5.2. Optical laser diode characterization	9
5.2.1. Output power and spectral characteristics	9
5.2.2. Beam profiling and size measurements	11
5.3. Construction of a biophotonic system	12

5.4. Brightfield and fluorescence imaging	14
5.5. Generation of convective flux	15
6. Results and discussions	16
6.1. Results of the output power and optical spectral characteristics	16
6.2. Results of the Beam profiling and size measurements	17
6.3. Imaging living microorganisms results	22
7. Conclusions	26
8. Future considerations	27
9. References	27

1. Introduction

In the life sciences, using only a biological or medical approach to understand organisms has proved to be insufficient. Thanks to physics the development of biology and medicine has grown because of technologies that are based on physical principles. Nowadays, for example, it is possible to use an ultrahigh resolving microscope to observe cellular structures smaller than 20 nm [1]. Another example is the Serial Femtosecond Crystallography (SFX) which offers the possibility of creating films of molecular transitions [2].

Recently, multidisciplinary research groups have been formed in order to investigate the behavior of living cells in laboratory conditions as close as possible to their normal environment. Physicists, chemists, biologists, and physicians can come together to try to understand the morphology, structure, metabolism, composition, signaling, reproduction and photoinduced effects in single cells. To study living cells, a widely common photonic tool system makes use of a microscope base where the required optical techniques can be incorporated simultaneously or individually. Optical techniques such as imaging, fluorescence, optical trapping and micromanipulation have been mostly used.

In particular, a multidisciplinary area of research that studies biological effects and phenomena with light is biophotonics. Generally speaking, biophotonics make use of optical techniques for studying molecules, single cells, and tissue in a non-invasive and sterile way. Thanks to novel biophotonic technologies such as fluorescence endoscopy and photodynamic therapy, it has been possible to recognize, much earlier, some types of cancer [1].

Lasers have been widely used in photonics and biophotonics [3]. Laser is an acronym for "Light Amplification by Stimulated Emission of Radiation". Lasers are well known for its directionality, coherence and brightness [3]. Because of its coherent property, it has also been used in biophotonics. At the Nippon Telegraph and Telephone (NTT) telecommunications energy Laboratories in Kanagawa, Japan, an optical system for monitoring blood flow was created. The system made use of a laser diode along with a photodetector on a silicon-based substrate [3]. In addition, Serial Femtosecond Crystallography uses a pulsed X-ray laser to generate video films [2].

Studies of motile living single cells such as flagellated microalgae placed in a small glass container with few tens of microns depth have been recently reported using an infrared laser [4]. On the other hand, limitations in the container size can cause adhesion of the cell flagella to the glass surfaces [5].

Reproducing environmental situation in a laboratory has been always difficult. In the case of microalgae cells, algal culture can be scaled from small, intermediate and large-scale containers [6]. The purpose of this work is to design and build a biophotonic system that will be used to study the behavior of motile biflagellated *Dunaliella tertiolecta* (Dt) microalgae in a bulk sample such as a cuvette of 10 mm (width) x 4 mm (depth) and 44 mm (height) with 0.75 mm wall size. Cuvette samples are normally used for spectroscopy

measurements [7] and recently a modeling microalgal flocculation and sedimentation [8]. As far as I understand, there are no studies of microalgae behaviors and photoeffects using these sorts of cuvette samples. The system will be composed of an illumination module, sample preparation module, and detection module. First of all, the observation of the Dt behavior will be using brightfield technique, which will allow having a large depth of focus for scanning the whole cuvette depth (4 mm). Moreover a fluorescence technique was incorporated into the system for studying both viability on adhered Dt cells on the cuvette walls and motility. For achieving the autofluorescence from the Dt cells, a Laser Diode (LD) source was electrically build and drive with an electrical circuit placed in a PCB (Printed Circuit Board). Due to the widespread use of a blue LD in life sciences research, a very complete optical characterization of the LD source was made. Measurements of the optical spectra as a function of output power, beam profile and size measure of the laser beam of emission was obtained hoping that these data would help to use this LD in some near future applications.

A CMOS camera was used for collecting the brightfield and fluorescence images. We report here the autofluorescence signal obtained from the Dt cells when a collimated laser diode of 407 nm was used for fluorescence excitation.

The biophotonic system composed of a long working distance objective lens, a 407 nm laser diode, a multi-axis translation stage, a computer, and a white light lamp. 25 frames per second recorded images were used for observing the behavior of the Dt cells.

Furthermore, as the LD is strongly absorbed by the microalgae and their living medium called F/2, an output power of 50 mW was focused inside the sample in the cuvette, which causes a convective flux observable by following the cells movility. The convective flux was induced by the photothermal heating.

This biophotonic system will be able to obtain either brightfield or fluorescent two-dimensional and three-dimensional images of a sample. One of the advantages of the system will be the simplicity of its construction and the capabilities to image inside the whole cuvette.

2. Background

For a better understanding of how to build a biophotonic system, three modules were considered: illumination module, a detection module, and a sample module. The biophotonic system will be used for imaging and video recording of living microorganisms in a cuvette and causing convective flux inside this cuvette by focusing strongly a high power blue laser diode.

2.1. Illumination Module:

The illumination module includes the material and devices used for achieving brightfield and fluorescence illumination. For brightfield a MR16 white light lamp and a

pinhole of about 4 mm open area were used. Fluorescent images were obtained by illuminating the sample with a collimated 407 nm laser diode beam.

2.1.1. Brightfield microscopy:

Brightfield microscopy is an illumination technique. This technique is commonly used in microscopes. For this technique a specimen is placed over the stage, the source of light (a lamp is usually used) is positioned so the light rays pass through the condenser. The light rays that pass through the sample, on the stage, go through the objective lens and forms an image in the eyepiece [7].

In a way, we have used a similar technique to illuminate the sample but without using any condenser. Instead, the light from the lamp were sent straight to the sample. A pinhole placed between the lamp and the sample helped to extend the depth of field inside the cuvette.

2.1.2. Fluorescence:

In this work it is desirable to observe fluorescent images from living microorganisms. Fluorescence is a process in which a molecule absorbs photons, thus it is taken to a higher energy level, and then returns to its initial energy state by releasing energy as photons. Fluorescence can be found naturally in green microalgae cells, this is called autofluorescence.

2.1.3. Laser diode (LD):

Ideally, a laser diode (LD) is a device which uses semiconductor materials to create a single wavelength light beam by using flux of electrons. The material of a semiconductor must be crystalline. Semiconductors are materials with conductivities between those of metals and insulators [9]. Metals, semiconductors, and insulators have what it is called valence and conduction band. These materials have a different energy gap (E_g) between these bands. The probability of an electron to jump from the valence band to the conduction band depends on the size of E_g . Figure 1 shows a diagram of the energy bands in a semiconductor. Usually, these materials are made of compounds found in group IV of the periodic table or a combination of elements from group III and V [9].

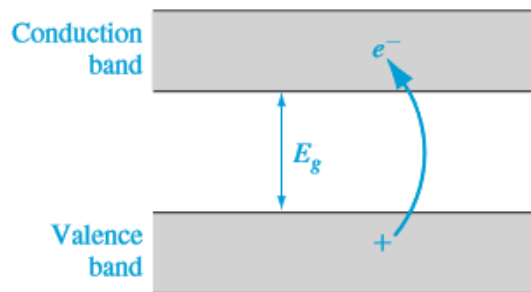


Figure 1. Energy band diagram, where E_g stands for Energy gap [9].

The addition of impurities on a semiconductor will create a semiconductor with an excessive amount of electrons (type n) or one with lack of electrons (type p). Being able to control the material's properties makes it useful for electronic devices. Interestingly, when combining "n" and "p" semiconductors, the result is a material with an n-p junction [9]. In the middle of the junction is a section called "depletion region" where there is a combination of electrons and holes. The depletion region has equilibrium of charge [9].

A LD works by using the depletion region on a semiconductor. After applying a biased voltage or current, electrons and holes start flowing towards this region making them recombine and create photons. Inside a semiconductor, there can be absorption and emission of photons and the emission can be either spontaneous or induced (see Fig. 2).

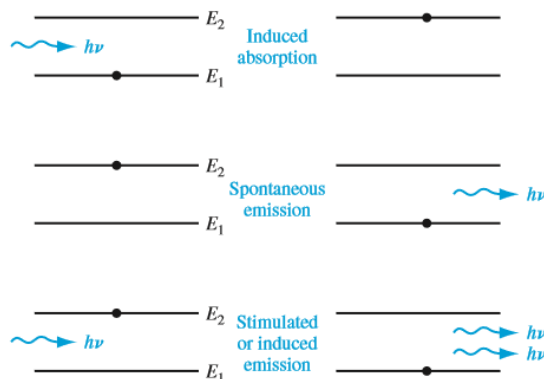


Figure 2. Schematic diagram showing induce absorption, spontaneous emission and induced emission [9].

As we can see in Fig. 2, in the case of stimulated emission, when a photon arrives to the semiconductor with an "electron" in the upper energy level (E_2), two photons are emitted when the "electron" decays to a lower energy level (E_1). This phenomenon is called optical gain or amplification. In addition to this effect and in order to create a laser beam from a semiconductor, a resonant cavity is also needed [3].

2.1.4. Laser diode optical characterization:

A blue laser diode of 406.5-407.5 nm wavelength was optically characterized. The important parameters to be determined were output power, optical spectra, beam profile and size of the beam.

The output power as a function of the operational current in the LD driver was obtained by using a power meter. The spectrum, for different currents, was obtained by a spectrometer which has a diffraction grating. A diffraction grating is an optical component with a periodic structure that diffracts and separate light into several beams with different directions. Gratings are commonly used on monochromators and spectrometers. Considering an ideal grating that reflects a plane wave of monochromatic light. The equation that relates the incidence angle, the direction of the rays, the slits spacing and the wavelength is:

$$d(\sin \theta_{diff} + \sin \theta_i) = m\lambda \quad (1)$$

where d is the slits spacing, θ_{diff} is the angle of the diffracted rays, θ_i is the angle of the incident ray, m is any integer and λ is the wavelength [10].

2.1 5. Spectrometer:

A spectrometer was used for the spectral characterization of the LD. The spectrometer is an instrument used to separate light into its different spectral components. Inside the spectrometer, there are mirrors, a grating, and a detector (see Fig. 3). An USB4000 spectrometer from Ocean Optics was used here [11]. Figure 3 shows the internal parts of the USB4000 spectrometer.

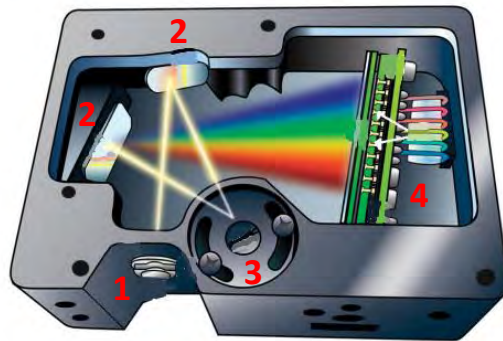


Figure 3. USB4000 schematic diagram, (1) Slit, (2) mirrors, (3) grating and (4) detector [11].

2.1.6. Use of Speckle pattern to find the laser diode's focal plane:

The LD used here has a lens mounted and by moving this it was possible to have a collimated or focused beam. We use the collimated beam to illuminate the Dt cells inside the cuvette for obtaining fluorescence images. A strongly focused high power LD beam was used to create a convective flux inside the cuvette with Dt cells. To be able to find the focal plane of the beam the speckle pattern was used. The speckle pattern is an interference pattern produced when coherent light reflects at a rough surface. It has been demonstrated that is possible to find the focal position of a laser by using the speckle pattern [12]. The size of the speckles is inversely proportional to the beam diameter and the rate of speckle motion is inversely proportional to the distance from the scattering object to the focus [12]. Knowing the last properties it is possible to find approximately the focal plane.

2.2. Detection Module:

Brightfield images of Dt cells can be obtained with a microscopic detection module composed of a collection lens of 50x microscope objective (long working distance infinity corrected objective) and a CMOS camera for displaying and recording the images.

In the case of fluorescent imaging detection, an excitation light source is required and the fluorescent emission must be collected. A 407 nm LD was used as an excitation source, and the fluorescent emission was obtained with the CMOS camera. An optical filter was used to block the light from the 407nm LD to pass the fluorescent light straight to the camera. This filter was located between the objective lens and the camera.

2.2.1. Infinity corrected microscope objective:

The system will use a Mitutoyo 50x infinity corrected objective lens to magnify the microscopic objects inside of the samples. This particular lens allows placing auxiliary optical components, such as optical filters, between itself and the detector or camera, without affecting the image formation [8]. Figure 4 shows a picture of the detection module where the infinity corrected objective was located.

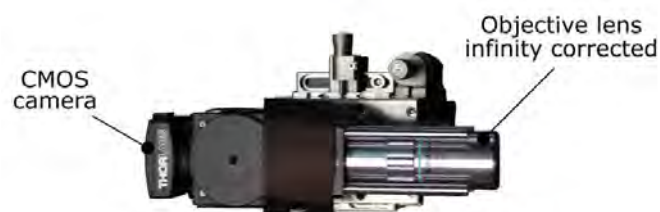


Figure 4. Detection system with an infinity corrected microscope objective mounted on a three-axis translation stage.

Initially, when an infinity corrected objective is used, the image of the magnified object could be found at several distances away from the back focal plane of this objective

without observing any significant changes in the image formation. Moreover one of the major advantages of this sort of objectives is that is possible to add optical filters between this objective and the image detector such as CMOS camera without affecting the image formation. The detection module also has a cube and an optical filter (it was placed inside the cube) was used for blocking the 407 nm LD beam and allow passing through the fluorescent light obtaining from the Dt cells.

2.2.2. CMOS camera:

The brightfield and fluorescent images were obtained with a complementary metal oxide semiconductor (CMOS) camera which uses a CMOS sensor. We used a DCC154M-GL ThorLabs with a resolution of 1280x1024 pixels, and a pixel size of 5.2 microns.

2.2.3. Optical Filters:

An optical filter is a component that transmits light within a range of wavelengths [13] while blocking the wavelength outside of this range. We used a long pass optical filter HQ530 LP M for blocking light of 407 nm and detecting fluorescent light from 530 nm up to 750 nm (see Fig. 5).

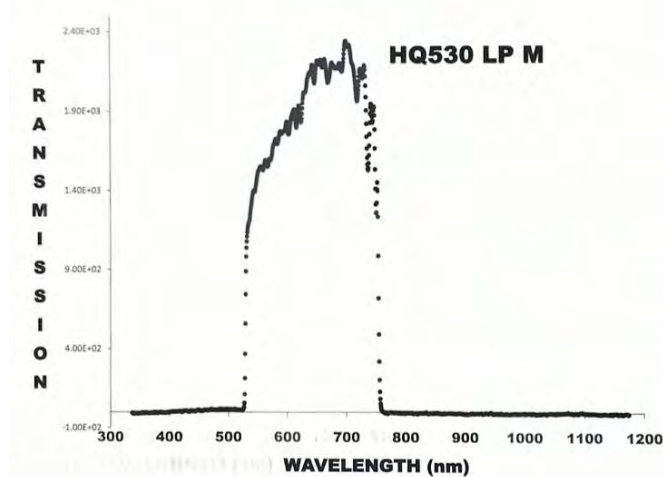


Figure 5. Transmission spectrum of a long pass HQ530 LP M filter.

It is worth mentioning that this filter was selected for avoiding the saturation of the CMOS camera when the LD beam was on, but must importantly to capture the fluorescent light from the Dt cells.

2.3. Sample Module:

A 3D (three dimensional) translation stage with 25 mm micrometers was used to hold the cuvette with Dt cells. This stage allows moving the sample in the space for selecting a specific volume to be imaged. The cuvette was mounted in a homemade plastic holder.

2.3.1. *Dunaliella tertiolecta* (Dt):

Dunaliella tertiolecta (Dt) is unicellular green algae. *Dunaliella* is well known for being responsible for primary production in hypersaline environments worldwide [14]. One example is the production of β -carotene. *Dunaliella* are able to produce β -carotene when they are exposed to stressful conditions such as salt environments, high intensity of incidence of light, high temperature and/or nutrients limitation [15]. The biophotonic system was created with the purpose of studying living microorganisms like the swimmers Dt microalgae.

2.4. Photothermal heating:

When a strongly focused high power laser diode beam is sent inside a cuvette with a liquid sample, thermal effects could happen. Heating a particular volume inside a sample can cause convective flux. Convection is a way of heat transfer. When a fluid is heated it starts generating movement of molecules from hot to colder zones [16]. In this work, convective fluxes, on a cuvette with Dt cells were studied. The forces exerted to the cells by the convective flux can be relevant, for instance, when cells are attached to the cuvette walls.

3. Hypothesis:

It is possible to develop a biophotonic system with a laser diode for imaging living microorganisms in a cuvette. Brightfield and fluorescent images can be obtained by illuminating the living microorganisms with a white light lamp and a 407 nm blue laser diode, respectively. Strongly focusing a 10 mW, 20 mW or 50 mW laser diode beam inside a cuvette filled with Dt cells sample, significant changes can be observed mainly caused for thermal heating.

4. Objectives

General Objective:

Develop a biophotonic system with a laser diode capable of visualizing living microorganisms in a cuvette, and imaging the changes obtained when a strong laser diode power is focused inside a liquid sample.

Specific objectives:

1. Capture and video record brightfield and fluorescent images of living *Dunaliella tertiolecta* cells in a cuvette.
2. Obtain and video record a convective flux caused by a strongly focused high power LD beam into a cuvette with living Dt cells.

5. Material and methods

For the construction of the biophotonic system, the following steps were made.

- 5.1 Electronic assembly of a laser diode
- 5.2 Optical laser diode characterization
 - 5.2.1 Output power and optical spectral characterization
 - 5.2.2 Beam profiling and size measurements
- 5.3 Construction of a biophotonic system
- 5.4 Brightfield and fluorescence imaging

5.1. Electronic assembly of a laser diode

A list of electrical and electronic components for assembly the LD driver on a PCB is shown in the Table I.

Table I. Material to assemble the LD driver and connect the LD.

Material	Details	Material	Details
Three resistances	7.5 Ω , 100 Ω and 1k Ω	Potentiometer	100 Ω
Diode	---	PCB	---
Aluminum Heatsink	---	Two capacitors	47 μ F and 0.1 μ F
Voltage Regulator	LM317	Voltage Source	12 V

First of all the electronic was assembled onto the PCB by soldering the above electrical parts. This was possible using the diagram provided by the supplier. Having the PCM ready, we then connected the LD as indicated. The laser diode was placed in an aluminum heatsink (as shown in Fig. 6) to allow static dissipation.

5.2. Optical laser diode characterization

5.2.1. Output power and optical spectral characteristics

The output power and the optical spectra of the LD for operation currents from 37.24 mA to 69.66 mA were obtained using the system shown on Fig 6. In this Figure, the LD beam was sent to a frosted glass (microscope slide) which was placed at $\sim 45^\circ$ of the incident beam, then a 90° of the direction of the beam a set of ND filters and the spectrometer (USB4000, Ocean Optics). A power meter (Spectra-Physics 405) was located between the LD and the frosted glass to obtain the output power for every current value set. We used YAMAMOTO Argon 488-514.5 nm laser goggles for eye protection. Before aligning the system shown in Fig. 6, the LD was started. For doing that, the LD driver was set to a minimum current by turning counterclockwise the potentiometer until reaching a resistance value of 12 Ω as indicated by the laser data sheet. The LD was then connected to the driver. A power supply of 8 volts DC was used to start the driver and thus to have the LD on.

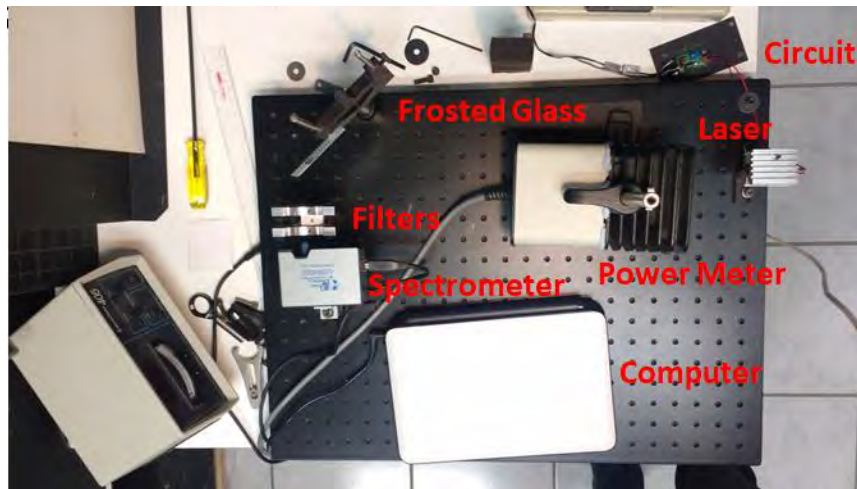


Figure 6. Setup used for output power and optical spectra measurements.

The alignment of the system was made using the minimum power (5mW) achieved by having a current of 37 mA in the LD driver. We carefully place the frosted glass, as indicated before, allowing some of the scatter light reaching the input of the spectrometer (see Fig. 6). When a signal with the spectrometer was obtained, the alignment of the system was done.

The data of the output power and spectrum for every current value set in the LD driver were taken following the next steps:

1. With the LD driver off, set the desire current value in the LD driver by turning CCW the potentiometer while measuring the resistance value with a multimeter. Remove the multimeter and then switch the LD driver on with 8 volts DC. Measure the output power by placing the power meter in the beam path. The maximum value on the power meter display was obtained by moving it up or down, left or right. The highest power value and the set current were the data taken
2. The power meter was then removed to allow the laser beam hit the frosted glass and get then the scatter light into the spectrometer. Neutral density filters were used to diminish the amount of light reaching the spectrometer thus avoiding any saturated signal. The measurement was recorded in a '.txt' document with the created computer program.
3. Switch off the LD driver by unplugging the power supply of 8 volts.
4. Repeat 1 to 4 steps for 5 different current values (37.24 mA, 42.18 mA, 51.88 mA, 61.08 mA, 69.66 mA).

5.2.2. Beam profiling and size measurements

We describe in this subsection how the beam profile or spatial mode of a focused LD beam was measured. Knowing the beam profile at different position away from the LD output, the beam size can be calculated. To know the spatial mode and the size of the beam at specific location, the Knife edge technique was used [17].

The approximately position of the focus of a LD beam was determined by using the setup on Fig 7. A LD beam was sent to a mirror and the reflected light was directed to a frosted glass mounted in a translational platform. The scattered light formed a speckle pattern that was observed over the screen. This pattern can be seen as the intensity pattern produced by the mutual interference of a set of wavefronts. Different patterns of light were formed depending of the position of the frosted glass through the focal plane of the LD. The size of the speckle interference is inversely proportional to the beam diameter (bigger speckle interference means smaller the beam size and thus being close to the focus) [12]. The focal plane then was roughly determined by observing the changes of the interference pattern while moving the frosted glass through the focal plane.

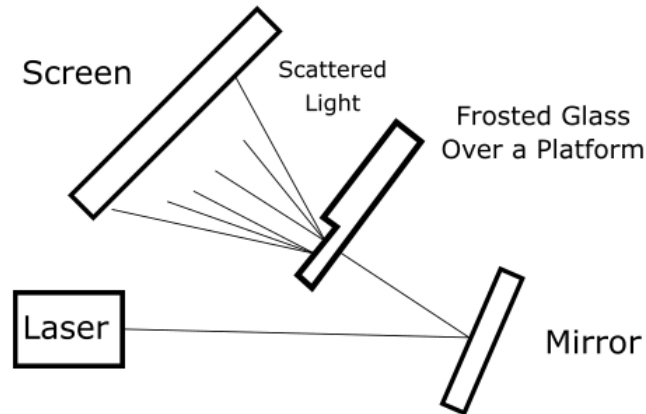


Figure 7. Setup used to find the focal plane of a focused LD beam.

Next, the Knife-Edge technique was used for measuring the beam profile at three different positions from the laser: 460 mm (before the focal plane); 545 mm (approximately at the focal plane), and 630 mm (after the focal plane).

Figure 8 shows the schematic of the knife-edge technique where the total output power of the LD beam was recorded as a knife or razor blade was translated through the beam using a calibrated translational stage. Here a razor blade was mounted on a two-axis translational stage with calibrated micrometers of minimum steps of 0.01 mm in both x- and y-axis and the LD power was measured with a Spectra Physics power meter. The power meter was connected to a multimeter which showed a voltage value for each power value.

For every single razor blade position, the value of the multimeter was taken. Data were taken for both horizontal and vertical direction. A homemade program was used for recording in a '.txt' file the voltage obtained for every single position of the razor blade. These data were displayed in a plot immediately after writing them. The data were taken until a constant value of the output LD power was reached. The data were then fit with an error function.

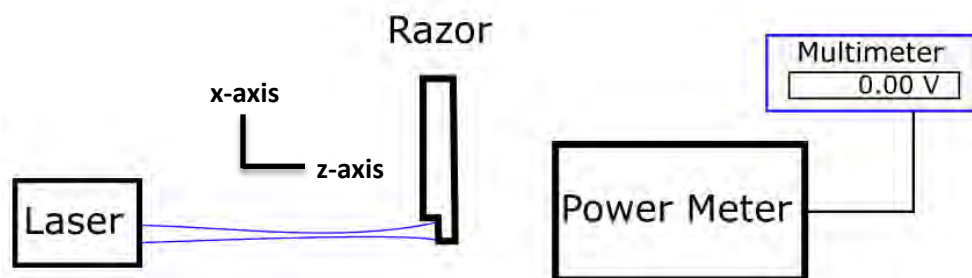


Figure 8. Schematic of the knife-edge technique for measuring the beam profile of a focusing LD beam.

5.3. Construction of a biophotonic system

The biophotonic system developed here consisted of three different parts called as illumination, detection, and sample modules. The three modules were placed together thus forming the biophotonic system developed here (see Fig 9).

5.3.1. Illumination module:

The illumination module was composed of a LD, a white light lamp, and a pinhole (see Fig. 9). These components were placed over an optical table as is shown in Figure 9. As we can see, the lamp was placed followed by the pinhole and then the sample to be studied.

The output intensity of the lamp was controlled with a 12 volts voltage supply device. Depending on the sample, the white light intensity was carefully selected for obtaining brightfield images with the correct brightness.

The LD beam was used as an excitation source for obtaining autofluorescent images from the living cells.

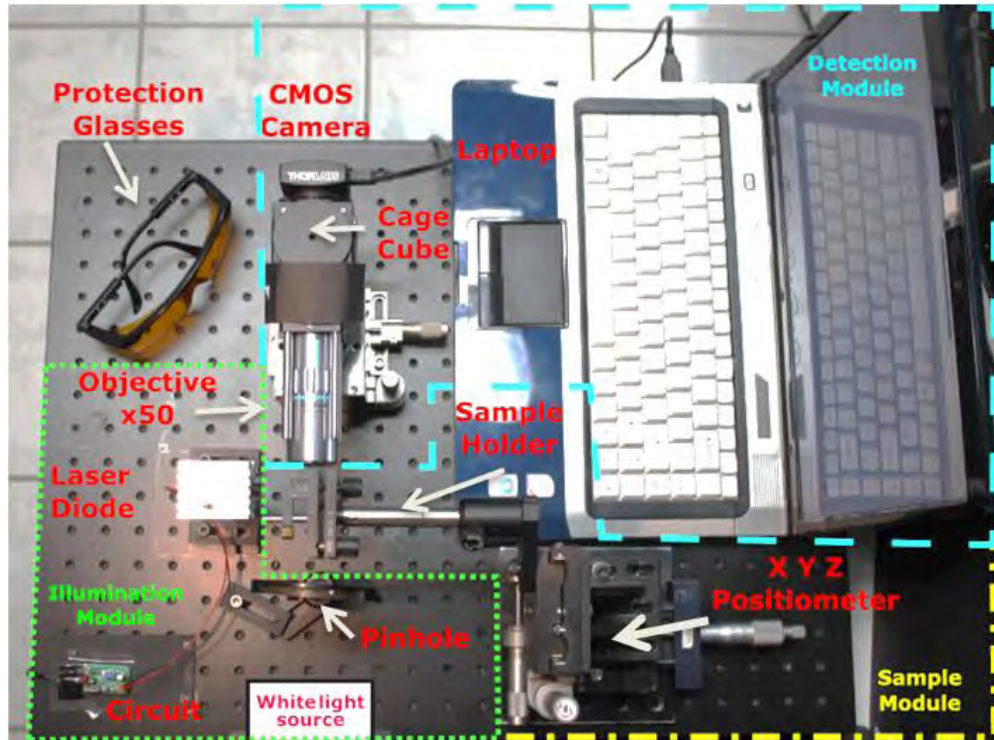


Figure 9. Biophotonic system comprising three modules: Illumination, sample and detection.

5.3.2. Detection module:

The detection module was composed of an infinity corrected objective, a long pass interference filter (HQ530 LP M), a CMOS camera, and a Laptop. This module was located atop of a three-axis translational stage for allowing taken images from everywhere inside the cuvette sample.

The CMOS camera was connected to the laptop via an USB port and was used with the software provided by the company.

CMOS camera position

Taking advantages of the infinity corrected objective lens, brightfield images were taken with the CMOS camera positioned at several distances away from the back focal plane of the infinity corrected objective.

Unfocused images were obtained when the CMOS camera was moved too far away from the objective. Moving the micrometers of the x-y-z translational stage, a recovery of the focused image could be obtained. When the distance increased between the camera and the objective lens, the image could get darker. The CMOS camera parameters in the software could be then used to increase the brightness at this point. After few small

adjustments, the camera was set at 100 mm away from the back focal plane of the objective.

5.3.3. Sample module:

The sample module is composed of a cuvette, sample holder and a three-axis translational stage for positioner the sample in a desire place. The translational stage was placed away from the other components to avoid blocking neither the white light lamp nor the LD beam. It was possible to move the sample in three dimensions. Once the sample holder was placed the cuvette was ready to be positioned.

5.3.3.1. Sample preparation:

Two types of samples were prepared, a thin chamber and a cuvette. The thin chamber samples were used for the initial tests on the Biophotonic system.

5.3.3.1.1. Thin chamber preparation:

A thin chamber of Dt was prepared as follow. First of all, a microscope slide was cleaned with propanol and Kimberly-Clark task wipers. A 50 μm thick spacer with a hole of 12 mm diameter was attached to the center of the slide. A 14 μl of the Dt cells sample was then poured into the hole avoiding any air bubble formation. Finally, a clean coverslip was placed atop the sample.

A histological sample of a human kidney (provided by the UABC) was also used for obtaining initial brightfield images. Both thin chambers of Dt cells sample and the histological sample were used to determine the proper position of the CMOS camera from the back focal plane of the microscope objective.

5.3.3.1.2. Cuvette preparation:

For the cuvette sample, 60 μl of Dt were added with the micropipette. The Dt cells were living in a $f/2$ medium [18]. The samples of Dt were provided by Dr. Beatriz Cordero, from the department of Aquaculture in CICESE.

5.4. Brightfield and fluorescent imaging:

Once the biophotonic system was built it was possible to observe the sample in real time with a recording rate of 25 frames per second. Brightfield images of three different samples were taken: a thin chamber with Dt cells in a stationary growth phase in a highly concentrated salt medium, a microscope slice of human kidney, and the cuvette with living microorganisms.

The microscope slice with the human rib was used for choosing the adequate distance of the CMOS camera away from the infinity objective lens. Pictures were taken at

different positions and some adjustments of the properties of the CMOS software as well as some refocusing of the detection module were made.

Field of view calibration

A brightfield image of a Dt cell in a thin chamber was obtained for calibrating the field of view. The position of this cell was located at the left edge of the image by moving the sample translational stage with a micrometer (the value of the micrometer was 4.90 mm). Then, the same cell was positioned at the right edge of the image (the value of the micrometer was 5.13 mm). The difference between these two measurements was 0.23 mm or 230 μm . The CMOS camera has a width of 1280 pixels thus every single pixel will give a measure of 0.18 μm in the detection system set here. In other words, if the number of pixels of an object in an image is known, then it could be possible to know the real size of the object.

Fluorescent images

Finally fluorescent images were obtained by adding the collimated LD beam to the system as an excitation source light. The fluorescent emission from the Dt cells was taken in a perpendicular direction from the excitation direction (see Fig. 9) to avoid as much as possible that the light from the LD beam reaches the CMOS camera. The interference filter was also added and placed between the infinity corrected objective and the CMOS camera for blocking the LD beam sent to the camera. Having a 9 mW output power from the LD, a cuvette sample with Dt cells was positioned into the system. The images and video were taken from several parts inside the cuvette.

5.5. Generation of convective flux:

The convective flux was possible to be observed by doing the follows. First of all, the white light illumination was used to obtain images inside the cuvette. When Dt cells were seen swimming at a speed of 150 microns/sec, then a strongly focused LD beam was sent towards the cuvette filled of highly concentrated Dt cells. An output power of 50 mW was initially used. Immediately after switching on the LD, the cells were seen to be pushed away by strong flux. This observation indicated the presence of convective flux. The event was video recorded at a rate of 25 frames per second. Changing the output power of the LD to 20 mW, the cells were seen to be still pushed but much slower than before. Finally, a power of 10 mW was used and the cells were just pushed very slowly by a weak flux. By moving the detection module across the whole cuvette, we could observe stronger drag forces exerted to the cells in a volume near the beam path, and also very weak drag forces away from the beam path and thus close to the walls.

6. Results and discussion

6.1 Results of the output power and optical spectral characteristics:

The Fig. 10 shows the output power of the LD as a function of the operational LD driver current. The values of currents used were from 37 mA to 70 mA. These data were fitted with a linear function.

Both coefficients R and R^2 are almost 1 meaning that the data in fact follow a linear behavior and has a positive slope. With this result is possible to know the power value that the laser will have by using a specific current, this is helpful to know when dealing with heat.

The corresponding optical spectra of the LD beam from the above operational LD driver are shown in the Fig. 11. Fig. 11 shows the data obtained (marks labels) by the spectrometer software and the Gaussian fit done for every set of data (continuous lines).

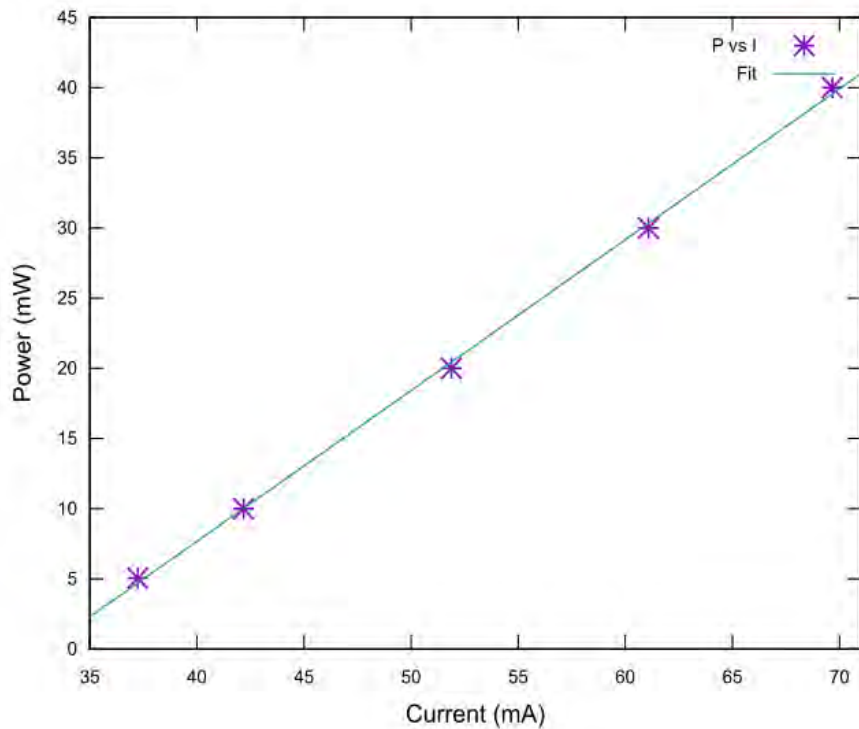


Figure 10. Output power of the LD beam as a function of operational LD driver current.

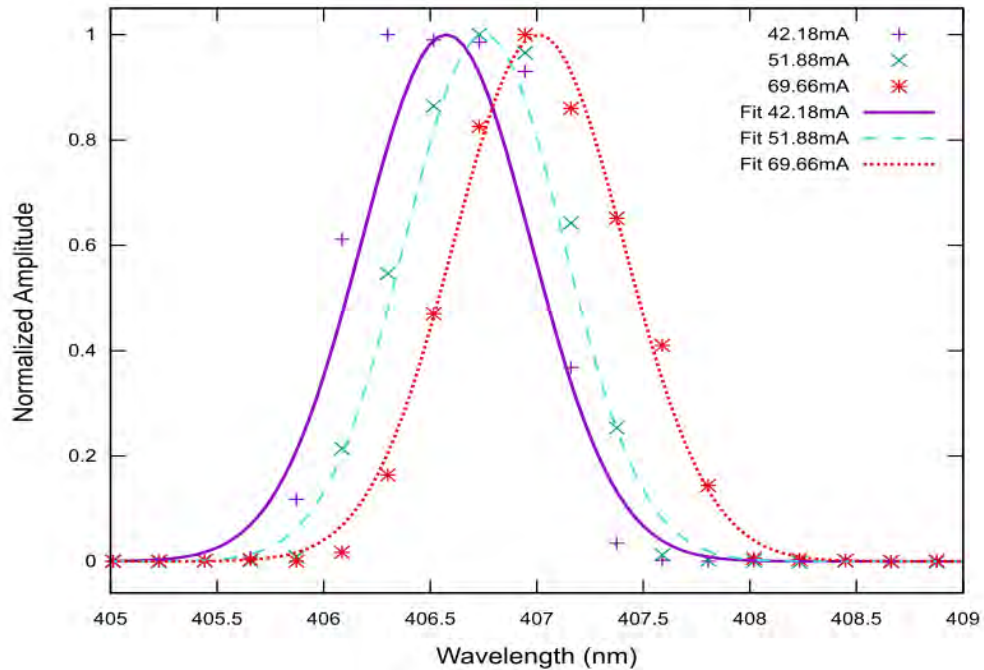


Figure 11. Optical spectra measurements of the LD, for three different driver currents.

The maximum value obtained for every fitted spectra are shown in Table II, where the data of the operational current for the LD driver (left column), wavelength peak (center column), and Spectrum width (right column) are shown.

Table II. Wave Length Peaks

Current (mA)	Wave Length Peak (nm)	Spectral Width or $\Delta\lambda$ (nm)
37.24	406.57	1.06
42.18	406.58	1.13
51.88	406.75	1.06
61.08	406.93	1.11
69.66	407.01	1.13

As it can be seen on figure 11, varying the driver current changes the peak position. A higher driver current gives a peak on a longer wavelength. This is an important result because it shows how sensible is the LD to driver current changes and is crucial to consider it when doing an experiment with a controlled environment.

6.2. Results of the Beam profiling and size measurements:

The measurements of the beam profile using the knife-edge technique were done for the vertical (Y-axis) and the horizontal (X-axis) direction perpendicular to the beam propagation (Z-axis) (see Fig. 8). The data obtained for three different positions (460 mm, 545 mm, and 640 mm) away from the LD output beam are shown below. Every plot was then fit with the error function such as erf(x).

The data shows on Fig. 12 and Fig. 13 are the data with their correspondent fit obtained at 460 mm away from the LD output.

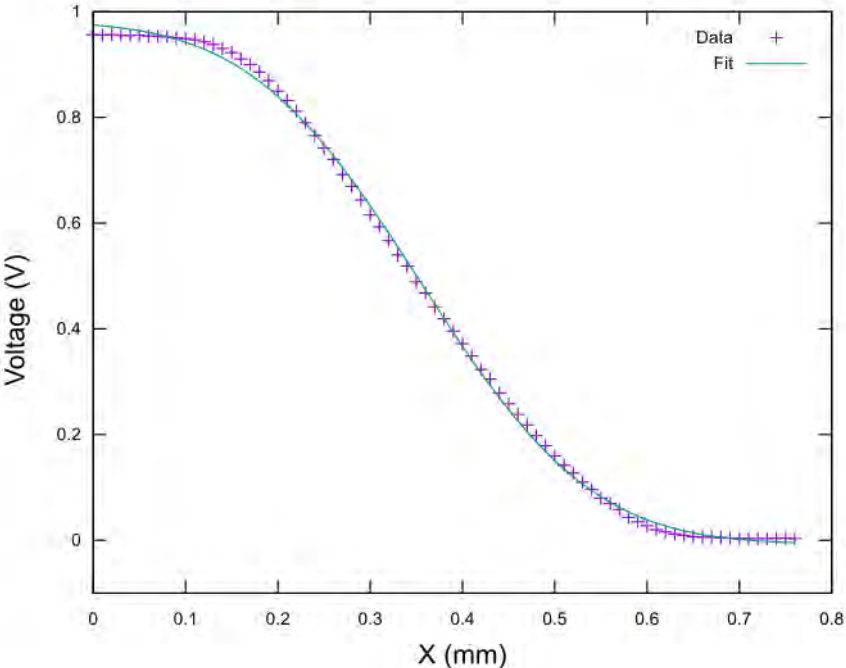


Figure 12. Razor blade position for X-axis at 460 mm from the laser.

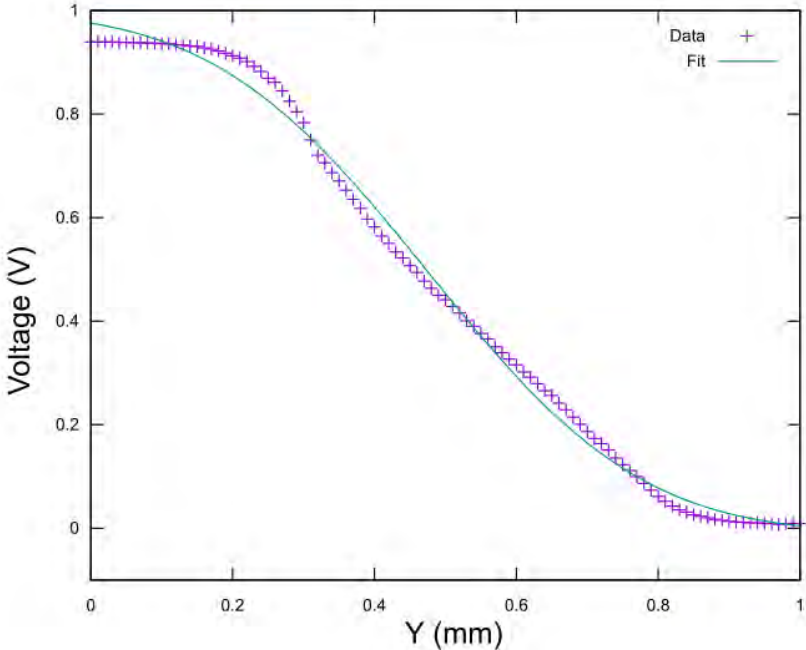


Figure 13. Razor blade position for Y-axis at 460 mm from the laser.

The data show in Fig. 14 and Fig. 15 are the data with their corresponding fit obtained at 545 mm away from the LD output.

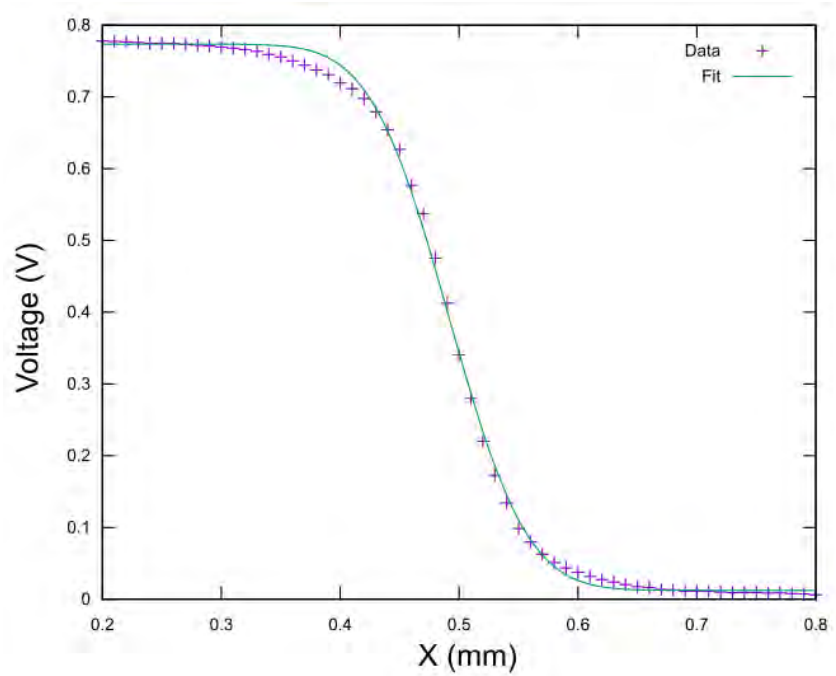


Figure 14. Razor blade position for X-axis at 545 mm from the laser.

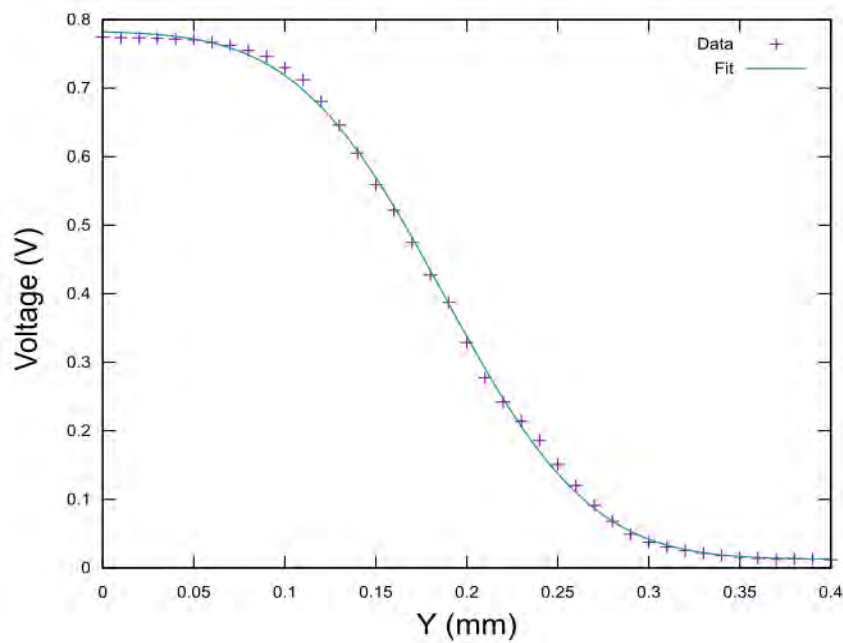


Figure 15. Razor blade position for Y-axis at 545 mm from the laser.

The data show in Fig. 16 and Fig. 17 are the data with their corresponding fit obtained at 630 mm away from the LD output.

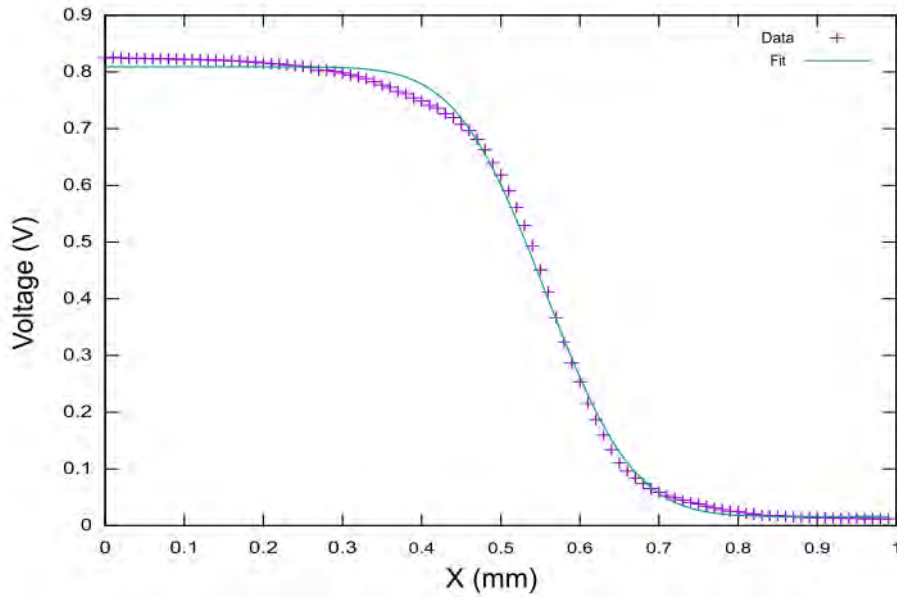


Figure 16. Razor blade position for X-axis at 630 mm from the laser.

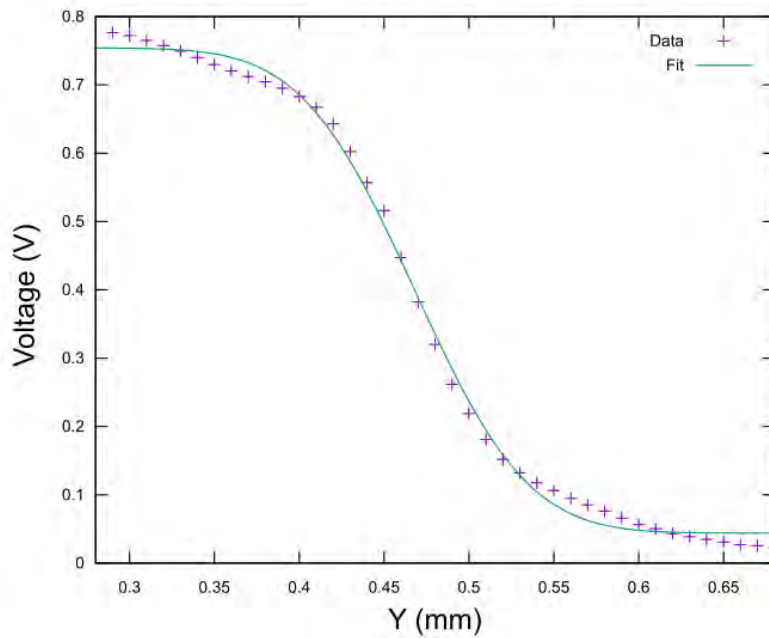


Figure 17. Razor blade position for Y-axis at 630 mm from the laser.

Qualitatively the X-axis graphs had very accurate fits; this is shown in Figs. 12, 14, and 16. As for the Y-axis, the resulting graphs Figs. 13, 15, and 17, showed qualitatively that the fit was not as accurate as the in the X-axis graphs. Qualitatively it can be seen that

the best fit for the Y axis was at the position 545 mm from the laser, this can be seen in Fig 15. With the fits, it was possible to obtain the laser width of all the three positions in both x and y-axis. Table III shows all of the widths in every position on both x and y-axes.

Table III. X and Y widths in every position.

Distance from laser (mm)	X width (mm)	Y width (mm)
460	0.58	0.95
545	0.20	0.25
630	0.35	0.26

By plotting the above results, the evolution of the beam can be seen in Fig. 18 where a spline fit was obtained to the corresponding data.

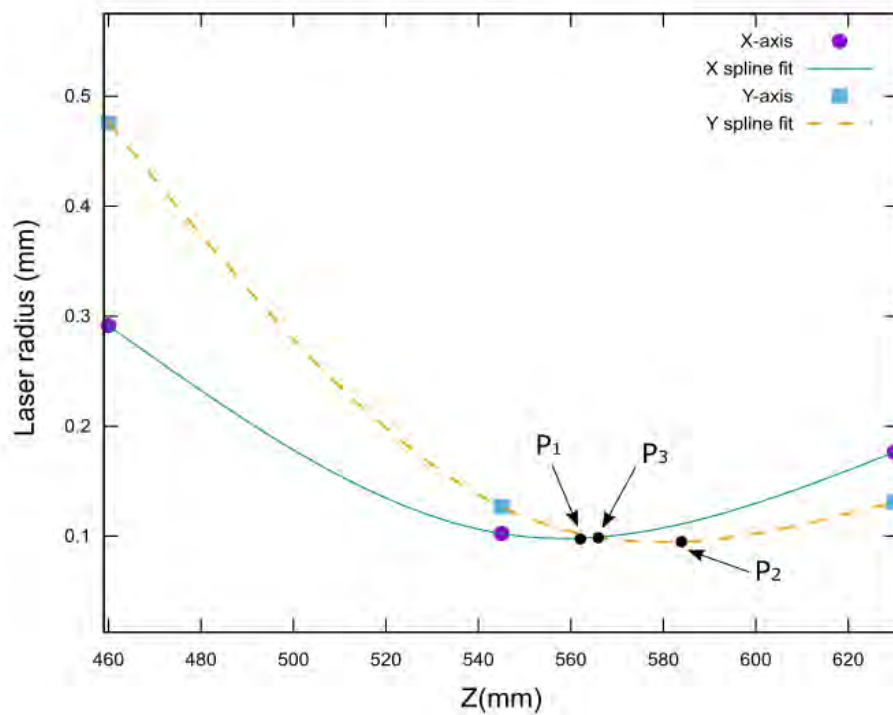


Figure 18. Evolution of the LD beam where $P_1(558,0.097)$ and $P_2(585,0.095)$ represent the beam waist in x-axis and y-axis, respectively and $P_3(566,0.099)$ is where the curves cross.

As seen in Fig. 18, the beam radius has its minimum value in x-axis at P_1 , and P_2 is the minimum value in y-axis. The intersection of the two curves represents the position where the beam has a circular profile of irradiance. These values describe a typical behavior of a focused LD beam.

6.3. Imaging living microorganisms results

Brightfield imaging from three samples:

A number of brightfield images were taken from thin chamber samples for the initial testing of the CMOS camera settings and the amount of white light illumination.

First, an image of a histological microscope slice of human kidney was obtained with the detection system (see Fig. 19). The image shows a fairly good contrast of the cells in the image for low amount of white light illumination. This sort of samples were very thin and thus easy to image.

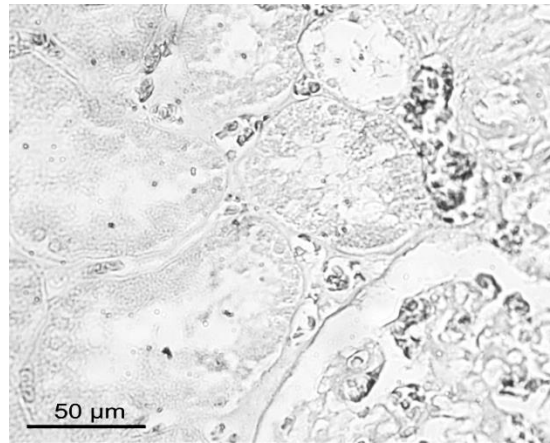


Figure 19. Brightfield image of a histological cut of human kidney using low amount of white light illumination.

Next, a brightfield image of a fairly dry *Dt* cells sample in a thin chamber (see Fig. 20). The image shows some “aggregations” of cells (dark areas) in what seems to be a drying medium with high salt concentration. The amount of white light used here was again minimal. The settings of the CMOS camera were kept similar than those used for Fig. 19.

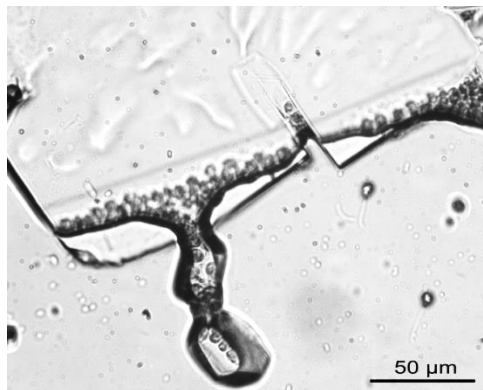


Figure 20. A dry sample of *Dunaliella tertiolecta* microalgae cells in a high salt medium.

The next step was to test the system with a cuvette. A cuvette sample filled with Dt cells at low concentration was located in the sample holder (see Fig. 9). The translational stage from the detection module was then moves until part of the cuvette was found. In this part, it is recommendable to increase the amount of white light illumination and open completely the pinhole, located between the white light lamp and the sample, for decreasing the depth of field to find a sharp image. After a while, eventually it was found cells adhered or immobilized on the cuvette wall (see Fig. 21). This image was used to set the properties of the CMOS camera using the software provided by the supplier. The settings to be adjusted were, among others, the pixel clock range, frame rate, and exposure time.

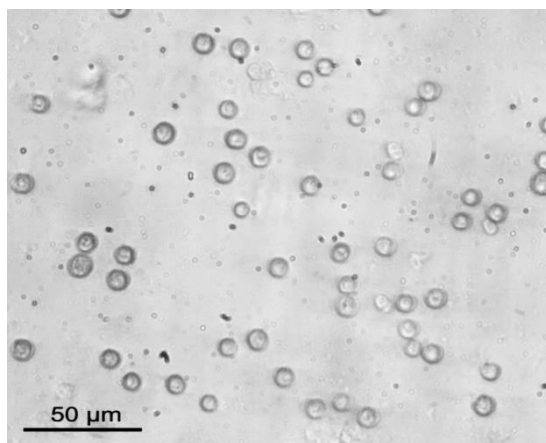


Figure 21. Dt cells immobilized on a vertical cuvette wall.

As seen, the built system was able to take brightfield images from a cuvette with fairly concentrated sample.

Videos of the sample with a high and low concentration of Dt

Brightfield images with a fairly small pinhole increases the field of depth thus for a high concentrated cuvette sample, an image of the wall cuvette can also show large areas of “shadows” from the cells located in different planes away from the wall (see Fig. 22(a)). The system was able to generate a clear image of the cells moving inside the cuvette with a low concentrated cuvette sample (see Fig. 22(b)).

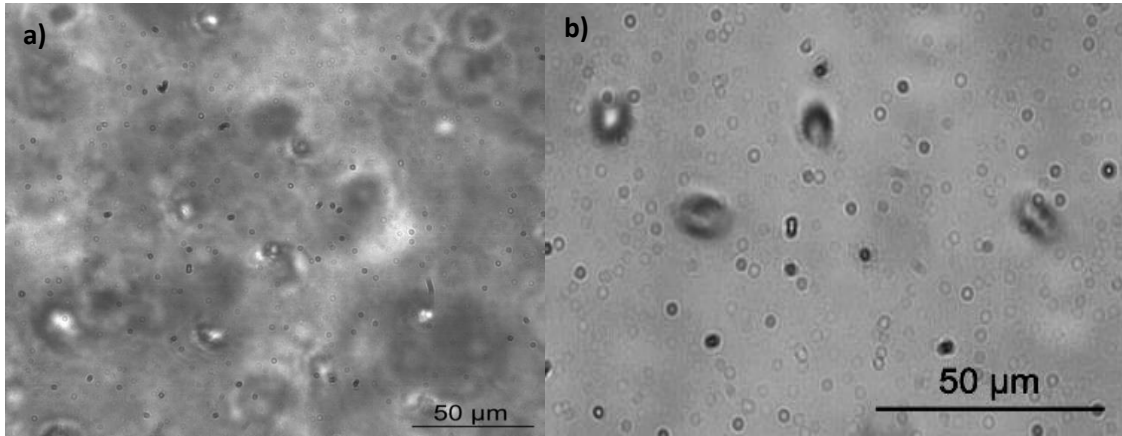


Figure 22. a) Sample with high concentration of Dt. b) Sample with low concentration of Dt cells.

Videos of Dt cells autofluorescence

A collimated LD beam was started with an output power of just 9 mW and sent it (in a direction perpendicular to the detection module) towards the cuvette filled with Dt cells (see Fig. 9). The long pass filter described before was placed between the infinity corrected objective and the CMOS camera, as it is shown in Fig. 9, for blocking the 407 nm LD beam and allowing detecting the autofluorescent light from the Dt cell bodies.

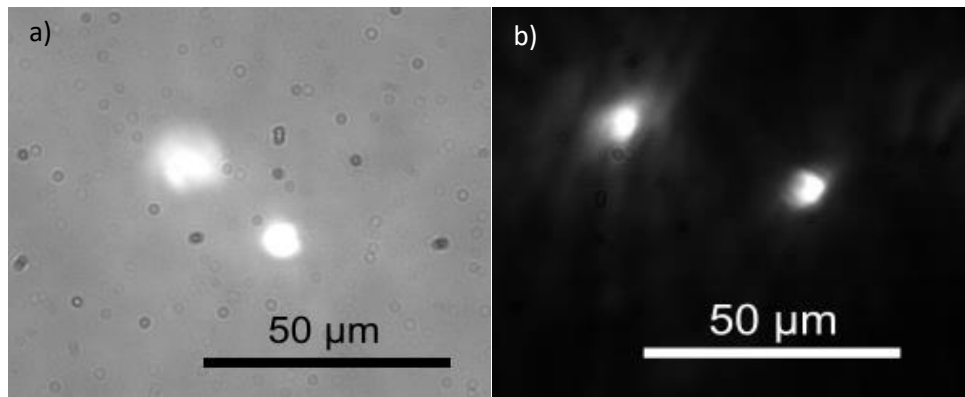


Figure 23. a) Fluorescence images from Dt cells with (a) white light illumination and (b) without white light illumination.

As the LD beam was illuminating just a small portion of the cuvette sample, the bright fluorescent light was obtained just in the volume where the LD was incident. A fluorescent image with also white light illumination is shown in Fig. 23(a), and a fluorescent image without white light illumination is shown in Fig. 23(b).

A peculiar pattern from the autofluorescent cells was an interesting observation. The pattern of light or the scattered light from some cell bodies had an “umbrella” shape. This

interesting observation was obtained when the illumination module was moving towards the LD following the beam path. Figure 24 shows the mentioned pattern.

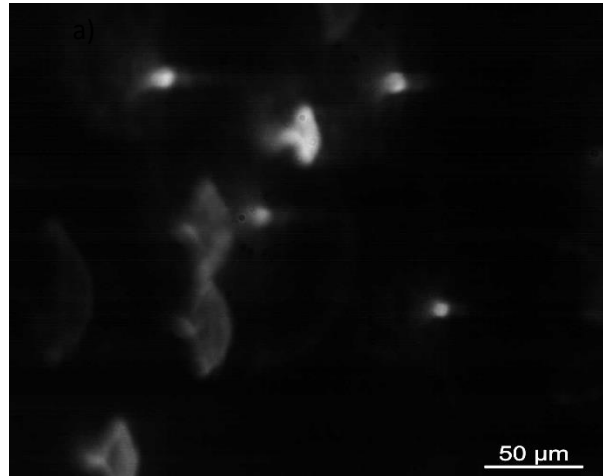


Figure 24. Peculiar umbrella pattern of the scattered light from the autofluorescence of Dt cells.

Convective flux

A convective flux was generated inside a highly concentrated Dt cell cuvette sample. This time the observations were made on a cuvette wall. Before starting the LD with an output power of 20 mW, an area with a cell attached to the vertical wall was found (see Fig. 25(a)). Then, we started the LD and, few second after that, a convective flux was observed, and then the amount of Dt attached on the wall was diminished. Figure 25 shows the wall of the cuvette before and after the generated convective flux. It seems that the attached forces were not very strong and thus the cells were removed from the wall when the medium was having a flux.

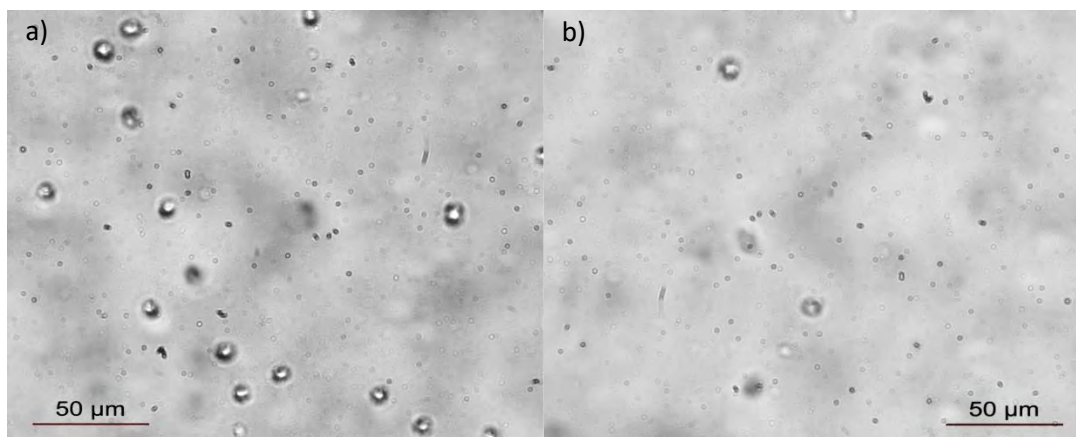


Figure 25. a) Fluorescent and brightfield images of Dt cells attached to the cuvette wall: (a) before generating a convective flux, and (b) after having a convective flux.

An interesting observation

Having a strongly focused 50 mW LD beam inside the cuvette filled with Dt cells, the formation of a sort of “speckle” pattern at a distance of 30 cm away from the cuvette could be observed. This pattern suddenly appeared and disappeared, it looked similar to a group of waves generated when throwing a rock in a pond. Figure 26 shows two images taken from a video of the observed pattern.

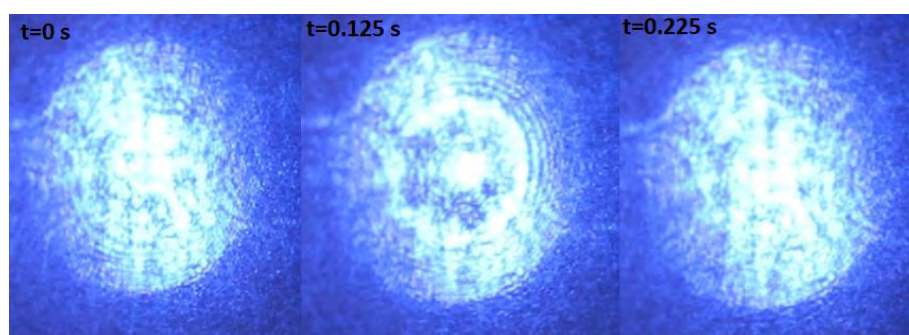


Figure 26. Three frames taken from a video showing the far field transmitted pattern of the LD beam after passing through the cuvette filled with a highly concentrated *Dunaliella tertiolecta* cells.

7. Conclusions

A biophotonic system with three modules was built. With this system, it was possible to observe samples on slides and inside a cuvette. Thanks to the camera and software not only images but videos were possible. A three-axis translational stage was used to observe a wide area of the samples and in the case of a cuvette sample; it was possible to look up to 4mm in deep with steps of every 1 micron. Knowing the size of each pixel can be used to know the size of the observed object by using proper software.

The CMOS camera could be placed at different positions away from the back focal plane of the infinity corrected objective lens. Depending on the position of the camera, few adjustments of the three-axis translational stage, of the detection system, or in the parameters of the image with the software were made to achieve an in focus image with corrected illumination.

When observing a sample in a cuvette it is more convenient to introduce a sample with no contaminants and with a small population, this way the generated image can be interpreted more accurately.

It was possible to obtain autofluorescent images and video from the Dt cells in a static and in a photothermal heated medium. The biophotonic system allowed taking brightfield and fluorescent images at the same time or separately.

Different scattered patterns from the autofluorescent light were observed. These patterns could be caused by an optical aberration (a defect in the obtained image) in the system or an effect caused by the angle and position of the Dt cells.

Strong convective flux was observed when using 20 and 50 mW. If observations without convective flux are needed, using low powers can be a solution but it will only decrease the force of the flux. It is important to consider that this force will be always present when heating a liquid. On the other hand, it was demonstrated that the convective flux can be used to detach the microalgae cells that were adhered to the cuvette wall, in this way the sample can be more homogeneous.

It is unknown what causes the pattern formed in the speckle pattern but because of its morphology, perhaps it was an indication of Dt cell aggregation near the beam path.

The system is simple and versatile, it can be used to study a great variety of samples and they can be in either a slide or a cuvette.

8. Future considerations

One of the advantages of the biophotonic system built here is its versatility and it is very compact. It is possible to add or remove components from it. In the system more optical techniques could be added, as for example, techniques of optical micromanipulation for holding a single cell inside a cuvette, but that will require expensive and more complicated equipment. Adding more advanced imaging techniques such as confocal laser scanning microscopy can be also possible but perhaps that will be difficult and slow task.

9. References

- [1] Jürgens, M., Mayerhöfer, T., Jürgen, P. (2011) HandBook of Biophotonics. Wiley Editorial, pages 1-38.
- [2] Fromme P., *et al.* (2017) Scientific American. Vol. 316 pages 62-67.
- [3] Hans Z. (2004) Laser Diode Microsystems. Springer, Berlin.
- [4] Ashkin A. (1991) ASGSB Bulletin Vol. 4(2) pages 133-146.
- [5] Beatriz Alina Juárez-Alvarez, et al, " "Studies of biflagellated microalgae adhesion using an optical trap system," Optical Trapping and Optical Micromanipulation XV, SPIE conference, 22 August 2018, San Diego, USA.
- [6] FAO (n/a) Funcionamiento del criadero: cultivo de algas. Food and Agriculture Organization of the United Nations, url: <http://www.fao.org/docrep/009/y5720s/y5720s07.htm>.
- [7] Bajhaiya A. K., Dean, A.P. Driver T., Trivedi, D. K., Rattray N. J. W., Allwood, J. W., Goodacre R., Pittman J.K., "High-throughput metabolic screening of microalgae genetic variation in response to nutrient limitation," *Metabolomics* 12:9 (2016)
- [8] Salim, S., Gilissen, L., Rinzema, A., Vermue, M.H., Wijffels R.H., "Modeling microalgal flocculation and sedimentation," *Bioresource Technology* 144, 602-607 (2013)
- [9] Abramowitz, M (2003) *Microscope basics and beyond*. Vol. 1, New York Microscopical Society.
- [10] Mitutoyo (2018) *Microscope units and objectives (UV, NUV, VISIBLE & NIR REGION)*. Catalog No. E14020, Mitutoyo.
- [11] Neamen, D. (2012) *Semiconductor Physics and Devices Basic Principles (4rd Edition)*. University of New Mexico.
- [12] Hecht, E. (2016) *Optics (5th Edition)*. Pearson Education.
- [13] Ocean Optics (2018) *USB4000 Fiber Optic Spectrometer, Installation and Operation Manual*. Ocean Optics, url: <http://oceanoptics.com/wp-content/uploads/USB4000OperatingInstructions.pdf>
- [14] Goodman J. W. (1976) "Some fundamental properties of speckle," *J. Opt. Soc. Am.*, Vol. 66, No. 11.
- [15] Kochengin, V. (2013) *Omnidirectional Optical Filters*. Springer.

- [16] Oren, A. (2005) A hundred years of *Dunaliella* research: 1905-2005. BioMed Central Ltd., Saline Systems.
- [17] Raja R., Hemaiswarya S., and Rengasamy R. (2007), "Exploitation of *Dunaliella* for β -carotene production," *Appl. Microbiol. Biotechnol.*, 74, pages 517-523.
- [18] Walker J. (2011) Halliday & Resnick: Fundamentals of Physics, 9na. edición, John Wiley & Sons, Inc., Estados Unidos de América.
- [19] Khosrofian J. and Garetz B. (1983) Measurement of a Gaussian laser beam diameter through the direct inversion of knife-edge data. *Applied Optics* Vol. 22, No. 21, pages 3406-3410.
- [20] Guillard, R. R. L. and Ryther J. H., "Studies of marine planktonic diatoms: I. *Cyclotella nana* (Hustedt) and *Detonula confervacea* (Cleve) Gran," *Can. J. Microbiol.* 8, 229-239 (1962).